Design against ship collisions in accordance with the new DNV RP C204

Jørgen Amdahl, Zhaolong Yu
Centre for Autonomous Marine Operations and Systems (AMOS), Norwegian University of Science and Technology (NTNU), Norway
Department of Marine Technology, Norwegian University of Science and Technology (NTNU), Norway.

ABSTRACT: A new version of the DNV RP C204 standard for the design of offshore steel structures against accidental loads was released in 2019. The updated recommended practice made considerable changes on the design against ship collisions. The changes addressed the challenge of increasing ship sizes and collision energy and new structural designs. This paper discussed several aspects of the changes in the revised DNV RP C204, including updated design collision energy and force-displacement curves of the standard supply vessel, ship installation interactions, compactness criterion of offshore tubulars and external dynamic models. Examples are given to demonstrate application of the new standards. Potential impact of the new standard on structural design is discussed.

Keywords: ship collisions; DNV-RP-C204 revision; ship platform interaction; compactness criterion; external dynamics

1 INTRODUCTION

The DNV RP C204 standard is a recommended practice released by DNV for the design of offshore structures against accidental loads. Accidental loads mainly include ship collisions, explosions, and fire. The overall goal in the design of a structure against accidental loads is to prevent an incident to develop into an accident disproportional to the original cause. This means that the main safety functions should not be impaired by failure in the structure due to the design accidental loads.

In the design against ship collisions, the size and speed of the vessel shall be determined by a risk analysis according to NORSOK N003 standard (NORSOK-N003, 2017), where the best estimate of a design impact event should not exceed an annual probability of occurrence of 10^{-4}. The standard collision event that has been used for the past several decades (DNV, 1981) is the impact from a supply vessel of 5000-ton displacement and a speed of 2 m/s. This gives a kinetic energy of 11 MJ and 14 MJ for bow/stern collisions and broad side impacts, respectively considering the added mass effects. Over the years, significant changes have taken place with noticeably larger ship sizes, increasing ship speeds and new structural designs (bulbous bows, X-bows, ice strengthen vessels, etc). Kvitrud (2011) summarized ship collision events on the Norwegian Continental Shelf in the period of 2001-2010 and highlighted six most severe cases, the collisions energies of which are in the range of 20-70 MJ. This exceeds significantly the standard collision energy in the old RP (DNV-RP-C204, 2010). In the revision of the NORSOK N-003 standard, the requirements to ship impacts were reassessed and updated based on statistics on supply vessel sizes and collision energies (Moan et al., 2017). The new NORSOK-N003 (2017) increased the standard design collision energy significantly to around 50 MJ. In consistent with the new NORSOK N003 standard, a revision of the DNV RP C204 standard (DNV-RP-C204, 2019) was released in 2019, where the design standards for ship collisions were rewritten. This paper discusses several new features of the new DNV RP C204 standard (DNV-RP-C204, 2019) for the design against ship collisions. Examples are given to demonstrate the application of the new standards. Potential impact of the new standard on the structural design is discussed.

2 UPDATED DESIGN ENERGY AND FORCE DISPLACEMENT CURVES

The latest NORSOK N003 (NORSOK-N003, 2017) standard requires that '*if no operational restrictions on allowable visiting vessel size are im-*

plemented, the displacement of supply ships should not be selected less than 10 000 tons from risk assessment. The corresponding speed in head-on collisions shall be set to 0.5 m/s and 3.0 m/s for ULS and ALS design checks, respectively. In sideways and stern impacts, the speed should not be less than 0.5 m/s and 2.0 m/s for ULS and ALS design checks, respectively. A hydrodynamic (added) mass of 40 % for sideways and 10 % for bow and stern impact can be assumed'. This yields a design collision energy of around 50 MJ, which represents a substantial increase from 11MJ and 14 MJ in the old recommended practice.

Design against ship collision is generally categorized into three regimes that depend on the relative strength. To dissipate a design energy of 11 MJ and 14 MJ following the old recommended practice, ductile design is often aimed for, where the bow or side of the striking ship is considered virtually rigid, such that most of the kinetic energy is dissipated by the impacted installation. However, an increase of the design collision energy to 50 MJ in the new RP places much heavier demands on the resistance and/or ductility of the offshore structure. It becomes difficult for the installation to absorb the energy alone without damaging structural integrity. It is therefore favorable that the striking ship also deforms and absorbs considerable energy. The relative strength then falls in the category of the shared energy design or strength design (see Fig. 1) depending on the amount of energy the striking ship dissipates.

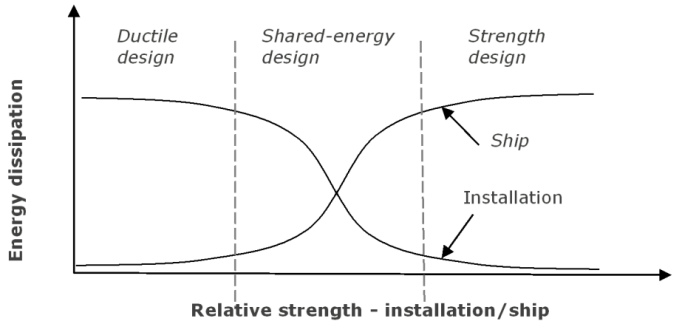

Figure 1. Energy dissipation for strength, ductile and shared energy design (DNV-RP-C204, 2019)

The new DNV-RP-C204 (2019) standard presented force-deformation curves for the selected standard supply vessels with a displacement of 6500-10000 tons for broad side, bow, stern end and stern corner impact (refer to Fig. 2). The bow deformation curve for raked bow without bulb may be used for the forecastle of supply vessel. The curves for broad side, stern end and stern corner impacts are based upon penetration of an infinitely rigid cylinder with a given diameter and may be used for impacts against jacket braces and legs (D = 1.5 m) and large diameter columns and plane side panels (D = 10m). It is clear that the force levels increase considerably compared to those from the old RP. For beam, stern end and stern corner impacts against jacket braces, energy dissipation in the OSV can be assumed provided that the brace has sufficient strength and the denting compactness requirement is complied with, see *Section 3*.

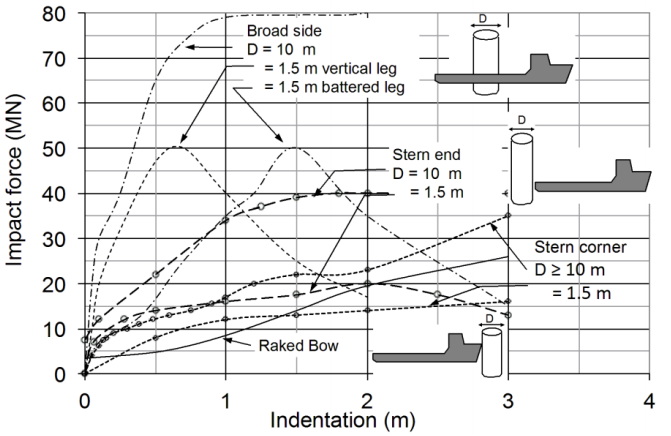

Figure 2. Recommended deformation resistance curves for beam, bow and stern impacts (DNV-RP-C204, 2019)

Bulbous bows and ice strengthened vessels are considered in the new RP. For supply vessels and merchant vessels with normal bulbous bows with no ice reinforcement or ICE-1C class and displacements in the range of 5000-10000 tons, the force deformation relationships given in Fig. 3 may be used for impacts against plane sides, circular columns and legs. It is noticed that even a modest ice class yields a significant increase of the collision forces (approx. 60%). For higher ice classes the increase will be even larger. If ice strengthened vessels collide with structures with no ice-strengthened structures, e.g. oil & gas platforms, pontoons of floating bridges, wind turbines etc., they will generally push the energy dissipation response into the ductile design regime.

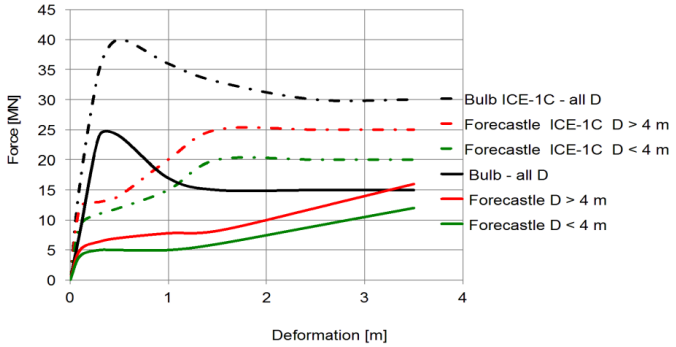

Figure 3. Force-deformation relationship for bow impacts from supply vessels with displacement 5000-10000 tonnes - standard bulbous bow with no ice-reinforcement and class notation Ice(1C) (DNV-RP-C204, 2019)

3 CROSS SECTION COMPACTNESS CRITERION OF TUBULAR BRACES AND LEGS SUBJECTED TO COLLISIONS

For ship collision with jacket structures, tubular braces and legs generally respond in three stages, i.e. local indentation, global bending, and axial stretch-

ing. Local indentation of cross sections will degrade significantly the load carrying capacity of tubular members in bending. According to the DNV-RP-C204 (2019) standard, for an indentation depth of 0.1D (D is the tube diameter), the reduction in plastic bending moment capacity due to local denting can be more than 30%. It is therefore desirable to maintain high compactness of tubular cross sections during collisions such that loading carrying capacity can be preserved.

In the old RP (DNV-RP-C204, 2010), braces are required to fulfill the compactness criterion $R_0 / R_c \le 6$ in order to avoid excessive local denting prior to forming a collapse mechanism, where R_0 is the plastic collapse resistance to bending and $R_c = 1/4\sigma_y t^2\sqrt{D/t}$ is a characteristic strength factor for local denting. σ_y is the material yield stress, t is the tube thickness, D is the diameter. Storheim and Amdahl (2014) carried out nonlinear finite element analysis of jacket braces and legs collided by a modern supply vessel and found that the compactness criterion $R_0 / R_c \le 6$ in the old RP can be overly conservative for most cases. They proposed to use the characteristic strength factor R_C as the new compactness criterion. Yu and Amdahl (2018a) and Yu and Amdahl (2018b) reviewed and discussed existing compactness criteria of tubular cross sections from the literature and found that $R_0 / R_c \le 6$ is equivalent to limit the *transition indentation ratio* $w_{d,tran} / D$ to a small value, where $w_{d,tran}$ is the indentation depth when tube deformation changes from local denting to global bending. This is proved to be insufficient to maintain cross section compactness. Yu and Amdahl (2018a) showed good performance of the R_c criterion by Storheim and Amdahl (2014) as the compactness criterion and proposed to relate R_c to the maximum collision force F_{max} when the ship crushes into a rigid brace/leg as follows:

$$R_c \ge 1.9\frac{F_{\max}}{24}\,(\mathrm{MN}) \qquad (1)$$

This is adopted in the revised DNV-RP-C204 (2019) standard as shown in Table 1. Here, the 24 MN corresponds to the maximum collision resistance for the standard supply vessel colliding into vertical braces or legs of 1.0-2.5 meters. 1.9 MN is the obtained R_c^* value for this scenario based on numerical simulations. R_c^* values for other impact scenarios are approximated by linear interpolation considering different possible F_{max} values.

For standard OSV bows with class ICE-1C, the factors R_c^* values shall be multiplied with 1.6 for impacts within the ice reinforced region and 1.25 above the ice reinforced regions. This corresponds to increased structural strengths and maximum collision resistance F_{max} values, as commented upon in Section 2.

Table 1. Required denting compactness R_c* values from DNV-RP-C204 (2019)

Ship type	Impact type	Denting compactness R_c* (MN)
Standard OSV with no ice reinforcment	Bulb vertical brace	1.9
	Bulb oblique brace	1.4
	Stern corner	1.0
	Side/stern end	1.2
Standard OSV with ice class ICE-C	Bulb or stern	3.2
	Side	2.3
V-shaped bow with ice Class ICE-C:	Bow on brace	3.5
	Leg and vertical brace	4.3
Other bow configurations	Bow on brace	$R_c^* = 1.9\frac{F_{\max}}{24}$
F_{max} = peak collision force if this occurs within 2 m deformation. Special considerations shall be taken when collision forces increase continuously.		

4 SHIP-PLATFORM INTERACTIONS IN COLLISIONS

The structural response of the ship and installation can formally be represented by load-deformation relationships as illustrated in Fig. 4. The strain energy dissipated by the ship and installation equals the total area under the load-deformation curves. As the load level is not known a priori, an incremental procedure is generally needed. The load-deformation relationships for the ship and the installation are often established independently of each other assuming the other object infinitely rigid. This method may, however, have severe limitations; both structures will dissipate some energy regardless of the relative strength. Often the stronger of the ship and platform will experience less damage and the softer undergoes more damage than what is predicted with the approach described above. As the softer structure deforms, the impact force is distributed over a larger contact area, for example, for a brace that is subjected to local denting. This is favorable for the ship because the contact area increases. The net effect is an "upward" shift of the resistance curve for the ship and less energy dissipation for the same load level as illustrated in Fig. 4.

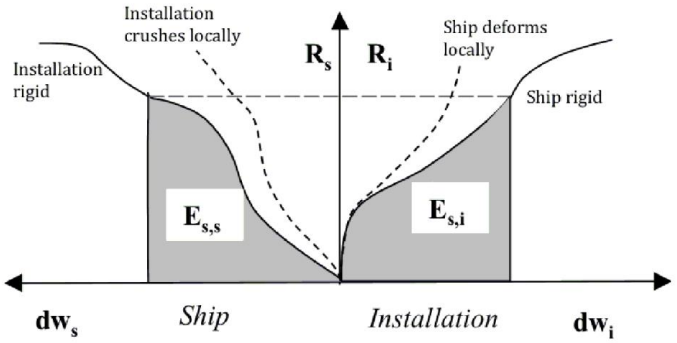

Figure 4. Dissipation of strain energy in ship and platform (DNV-RP-C204, 2019)

In the new DNV RP C204 (DNV-RP-C204, 2019), this interaction effect is taken into account by defining a correction factor β which depends on the re-

sistance to local denting/flattening for tubular members and local shear buckling or torsional buckling for stiffened plates

$$E_s = E_{s,s} + E_{s,i} = \beta \int_0^{w_{s,\max}} R_s dw_s + \int_0^{w_{i,\max}} R_i dw_i, \quad 0 < \beta < 1 \qquad (2)$$

where $\beta = R_c / R_c^*, \max 1.0$ for impacts against tubular members. R_c and R_c* are defined in Section 3. For vertical brace impact on supply vessel bows with a diameter of 1 m and a material yield stress of 355 MPa, the thickness required to get a β factor of 1.0 is 77 mm for bulb impact on vertical brace from standard OSV with no ice reinforcement bulb impact on vertical brace, but wholly 109 mmm for ICE 1C reinforcement. For ship collisions with stiffened plating, β is defined as $\beta = Z_r / Z_p^*, \max 1.0$, where Z_r is the average plastic modulus along the stiffener and Z_p^* is the minimum required plastic section modulus.

Take stern end impact simulations on tubular members from Yu and Amdahl (2018a) as an example. The stern end is from a standard modern supply vessel of 7500 tons, see Fig. 5. The struck tube has yield strength of 285 MPa, a length of 20 m, a diameter of 1.5 m and varying thicknesses. For stern end impacts, the compactness criterion requires a R_c^* of 1.2 MN.

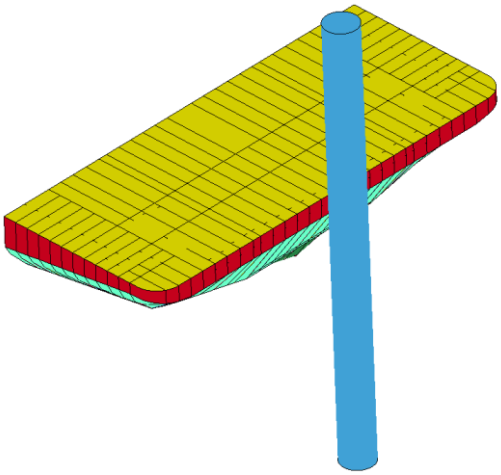

Figure 5. stern end impacts on tubular braces (Yu and Amdahl, 2018a)

Fig. 6 shows the simulation results using the nonlinear finite element code LS-DYNA (Yu and Amdahl, 2018a) with different tube thicknesses. For a tube thickness of 30 mm, $\beta = R_c / R_c^* = 0.375$ and the energy dissipated by the ship is substantially reduced by 62.5% according to Eq. (2). From the simulation results in Fig. 6, it is observed that the tube is very weak and energy dissipation of the ship is virtually zero, so the RP is somewhat non-conservative. For a tube thickness of 60 mm, we obtain $\beta = R_c / R_c^* = 1.07$ and $R_0 > F_{\max}$, and this yields ductile design with a virtually rigid tube according to the RP. This is consistent with simulation results. Shared energy in both the ship and the installation occurs for tube thickness varying from 40 mm to 55 mm. This represents a relatively narrow shift from ductile design to strength design. Simulation results from Fig. 6 show clearly the upshift effect of the ship resistance with tube deformation.

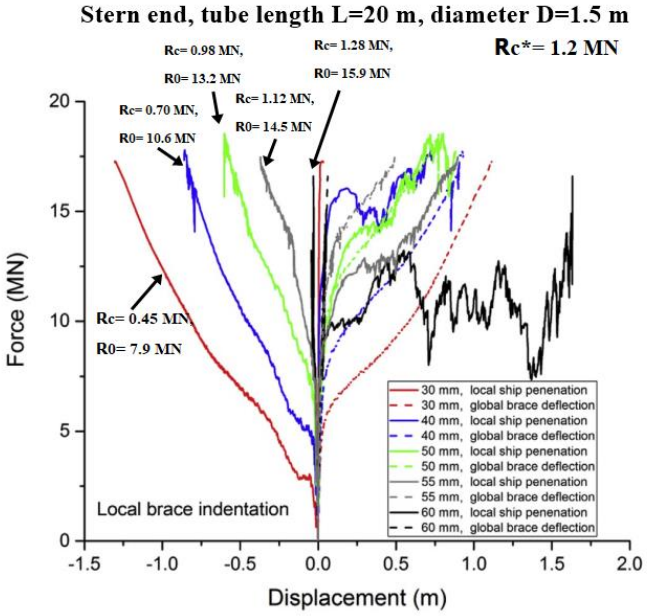

Figure 6. Force versus local indentation and beam deformation of braces and force-versus penetration of stern end-vertical brace with 1.5 m diameter and varying thicknesses, from Yu and Amdahl (2018a)

It is clear that the introduced β factor in Eq. (2) by DNV-RP-C204 (2019) is a simple way of considering ship-installation interaction by assuming linear decrease of ship energy dissipation with respect to decreasing compactness. For numerical simulations, the interaction trend by Eq. (2) is well captured. The energy share in the ship and the installation is, however, not simply linear. It depends on the total energy to be dissipated and the shift region of their relative strength by varying tube thickness is relatively narrow.

5 EXTERNAL DYNAMICS

In the general case, considering impact normal to a defined impact plane, the dissipated energy will have contributions from the relative motions tangential to- and normal to the impact plane. Disregarding the energy dissipated tangentially ("friction" energy), the energy dissipated in normal direction may be obtained as follows

$$E_{str} = \frac{1}{2}\bar{m}_s \bar{v}_s^2 \frac{\left(1 - \frac{\bar{v}_i}{\bar{v}_s}\right)^2}{1 + \frac{\bar{m}_s}{\bar{m}_i}} \qquad (3)$$

where $\bar{v}_s$ and $\bar{v}_i$ are the velocity of the ship and the installation, respectively, taken normal to the impact plane (the signs are equal when moving in the same direction). The equivalent mass, $\bar{m}_j$, for the installation and the ship, respectively, depends on the corresponding

mass, and mass moment of inertia, $\bar{I}_{jx}, \bar{I}_{jy}, \bar{I}_{jz}$, about the three axes of the coordinate system including hydrodynamic added mass, all projected on the collision plane and is given by (Popov et. al. (1967):

$$\bar{m}_j = \left(\frac{l_j^2}{\bar{m}_{jx}} + \frac{m_j^2}{\bar{m}_{jy}} + \frac{n_j^2}{\bar{m}_{jz}} + \frac{\lambda_j^2}{\bar{I}_{jx}} + \frac{\mu_j^2}{\bar{I}_{jy}} + \frac{\nu_j^2}{\bar{I}_{jz}} \right) \qquad (4)$$
$$j = s \text{ (ship)}, = i \text{ (installation)}$$

The collision point is described by the three coordinates (*x, y, z*) relative to the center of gravity for the installation and the ship. *l, m, n* are the direction cosines for the unit vector normal to the collision plane (pointing outwards) where the location of the contact point is expressed in the two coordinate systems

$$P\left(x_j, y_j, z_j\right), \quad \mathbf{I}_j = l_j \mathbf{i} + m_j \mathbf{j} + n_j \mathbf{k}; \qquad (5)$$
$$j = s \text{ (ice)}, = i \text{ (installation)}$$

The lever arms for roll, pitch and yaw motions are given by:

$$\begin{aligned} \lambda_j &= mz_j - ny_j \\ \mu_j &= nx_j - lz_j \\ \nu_j &= ly_j - mx_j \end{aligned} \qquad (6)$$
$$j = s \text{ (ship)}, = i \text{ (installation)}$$

The calculation of the above parameters shall be performed for both the ship and the installation using a uniquely defined impact plane. The orientation of the collision plane is not always obvious. Normally, the stronger side, or the object with a flat surface or a convex outer shape at the impact point shall be used as the master object to establish the local coordinate system (especially the normal direction). The averaged normal direction can be used when it is difficult to choose direction.

The tangential motion components on the collision plane related to 'friction' energy dissipation may also be taken into account using the complete 3D model developed by Liu and Amdahl (2019). This method considers two outcomes of the collision event, depending on the amount of friction forces along the collision plane, namely i) slide, where the two bodies move tangential to the collision plane, ii) stick, where the two bodies stick together. The sliding case with friction set to zero condensates into the solution given by Popov et. al. (1967). The friction factor should take into account coulombic friction as well as any transverse force due to deformation in the tangential direction. This force component is generally smaller than the force caused by pure lateral indentation.

The installation can be assumed compliant if the duration of impact is small compared to the fundamental period of vibration of the installation. If the duration of impact is comparatively long, the installation can be assumed fixed. Floating platforms (semi-submersibles, TLP's, production vessels) can normally be considered as compliant. Jack-ups may be classified as fixed or compliant. Jacket structures can normally be considered as fixed.

If we consider a ship that is drifting sideways impacts a floating structure with the bow, the ship will be subjected to impulses in sway and yaw. Conversely, the platform may be subjected to an impulse in sway and roll/pitch. We may express the effective masses in Eq. 3 as:

$$\begin{aligned} \bar{m}_s &= m_s \left\{ 1 + \left(\frac{x_s}{r_s} \right)^2 \right\}^{-1} = m_s \left\{ 1 + x^2 \right\}^{-1} \\ \bar{m}_i &= m_i \left\{ 1 + \left(\frac{z_i}{r_i} \right)^2 \right\}^{-1} = m_i \left\{ 1 + z^2 \right\}^{-1} \end{aligned} \qquad (7)$$

where x_s is the longitudinal coordinate of the impact point with the coordinate origin at the ship center of gravity and and r_s is radius of gyration for yaw of ship and z_i and r_i are the vertical coordinate of the impact point and radius of gyration in pitch/roll of the platform. It is observed that a key parameter for inducing angular motion are the levers measured in terms of the radii of gyration. The larger the levers, the less is the effective masses, when they are equal to unity, the effective masses are reduced by 50%.

The demand for energy dissipation as a fraction of ship kinetic energy is plotted as a function of the effective mass ratios of the ship and the platform in Fig. 7. The upper curve for x = 0, z = 0 relates to central impacts, i.e. the force vector goes through the center of gravity of both structures and no rotation occurs. For $m_s/m_i<1$, the platform mass is larger than the ship mass and the demand for strain energy dissipation relative to initial kinetic energy E_{str}/E_0 is large. This is representative in many cases for fixed platforms. When the ship mass is much larger than the platform mass, the fraction goes towards zero. Even if the fraction is small, the demand for energy dissipation may be large if the ship mass is large (e.g. a super tanker).

It is observed that the influence of the lever for the ship (x >0, z =0) on strain energy absorption is significant when the mass ratio is small but diminishes when the mass ratio is large. Conversely, the lever for the platform must be relatively large, i.e. z > 0.5, to be of significance. Its effect increases for large mass ratios. In general, it may be stated that the effect of rotation may be neglected for small levers, i.e. x, z < 0.25.

Popov et al. (1969) parametrized radii of gyration of typical ship. The radius of gyration in pitch and sway will be in the range of $0.25L_{pp}$ where L_{pp} is the length between perpendiculars. Thus, the maximum value of x is around 2. The radius of gyration in roll is $r_x \simeq 0.3\left(B^2 + D^2\right)$ where B = ship breadth and D= ship depth. In the midship area, the lever will often

be small, but it may be relatively large in the foreship area, as the forecastle deck may be located high above the center of gravity. Yaw, pitch and roll may occur substantially, and the equivalent mass may become significantly smaller than the translatory mass.

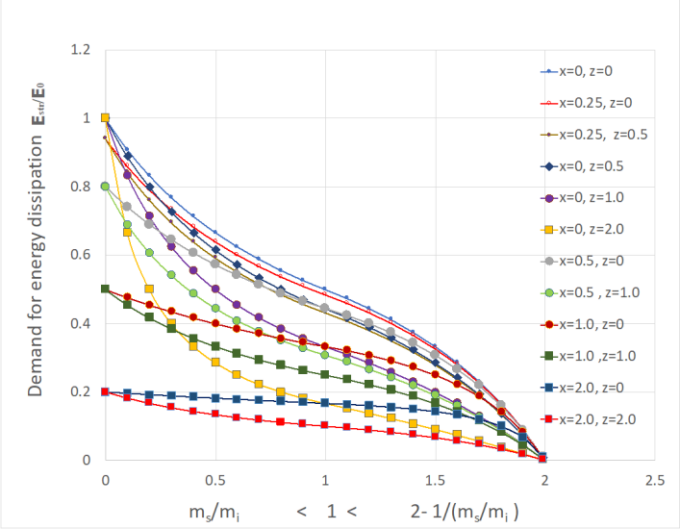

Figure 7. Ratio of strain energy dissipation relative to the initial kinetic energy versus different mass ratios and relative positions

An example application for ship collisions with floating offshore winds is given here using USFOS simulation results from Yu et al. (2021). The striking ship is a characteristic shuttle tanker with a displacement of 150,000 tons. The floating turbine has a three-column semi-submersible floater and the total mass is 23610 tons. The tanker side is given an initial impact velocity of 2 m/s corresponding to a kinetic energy of 420 MJ.

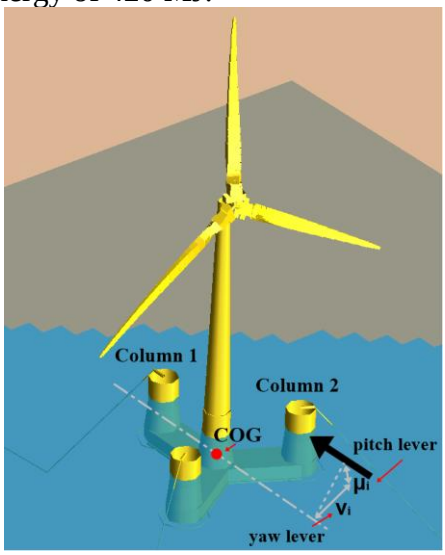

Figure 8. Tanker collision with a submersible floating offshore wind turbine from Yu et al. (2021)

For tanker side collision on column 1, the resulting strain energy dissipation is 56.7 MJ from external dynamics versus 58.9 MJ from USFOS simulation, which is reasonably accurate. The surge and pitch motions contribute 96.4% and 3.6% to the dissipated strain energy respectively. The pitch motion contribution is quite limited. For tanker side collision on column 2, the external dynamic model predicted reasonably well a strain energy dissipation of 27.8 MJ versus 30.5 MJ obtained with USFOS. The yaw, surge and pitch motions contribute 54.4%, 44.0 % and 1.6% to the strain energy absorption, respectively. This shows the importance of the yaw motion in non-centric impacts. More details can be found in Yu et al. (2021).

6 FORCE-DEFORMATION RELATIONSHIP OF BEAMS CONSIDERING BOUNDARY AXIAL FLEXIBILITIES

DNV-RP-C204 (2019) updated formulations for the plastic force deformation relationship of beams considering boundary axial flexibility. This is in general consistent with the detailed derivation in Yu et al. (2018) for beams with stiffened plating cross sections. The results showed that relatively small axial displacements have a significant influence on the development of tensile forces in members undergoing large lateral deformations, see Fig. 9.

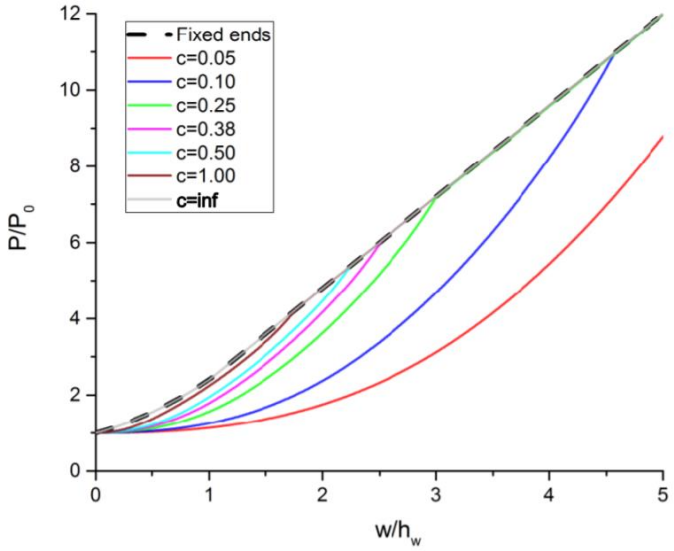

Figure 9. Resistance-displacement curves for a beam with stiffened plating cross section given different translational stiffnesses (Yu et al., 2018)

7 CONCLUSIONS

This paper reviews the changes of the newly released DNV RP C204 standard for the design of ship collisions and discuss their application and impact. The standard design energy was significantly increased from 11 MJ and 14 MJ for ship bow and side collisions respectively to 50 MJ. This in general requires that the ship also deforms and absorb considerable energy, where the ship platform interaction effects can be important. The effects are considered simply by introducing a β factor. This is shown to capture the general trend by comparison with numerical results, but the energy share in the ship and the

installation is however not simply linear. The transition zone from strength design to ductile design is relatively narrow.

Tubular braces and legs should fulfill compactness criterion of cross sections so as to avoid excessive local indentation and subsequent degradation of load carrying capacity. The new RP adopts the R_c factor as an indicator instead of R_0/R_c in the old version. This is shown to work well by comparison with numerical simulations.

If more accurate assessment of the ship and the hit structure is desired using Abaqus or LS-Dyna, DNV offers shell-based FE models of standard supply vessel bows and stern ends that may combined with FE models of the hit structure.

The simple formulations used in the external dynamic models give quite good accuracy in predicting the energy dissipation. The *square of the lever over radius of gyration ratio* is shown to govern the contributions of the associated motion to the equivalent mass, and subsequently the strain energy absorption.

Formulations for the plastic force deformation relationship of beams were updated considering boundary axial flexibility. It shows that relatively small axial displacements have a significant influence on the development of tensile forces in members undergoing large lateral deformations and should be carefully accounted for.

ACKNOWLEDGEMENT

The authors gratefully acknowledge the financial support by Research Council of Norway via the Centers of Excellence funding scheme, project number 223254 – NTNU AMOS. The authors would also like to thank the support from high performance computation resources from the Norwegian national e-infrastructures, Project NN9585K - Accidental actions on strait crossings and offshore platforms.

REFERENCES

DNV-RP-C204 2010. DNV-RP-C204: Design against accidental loads. *See http://www. dnv. com*.

DNV-RP-C204 2019. DNVGL-RP-C204 Design against accidental loads. *DET NORSKE VERITAS*.

DNV 1981. Impact loads from boats. *Technical Note for Fixed Offshore Installations TN A*, 202.

KVITRUD, A. Collisions between platforms and ships in Norway in the period 2001-2010. ASME 2011 30th International Conference on Ocean, Offshore and Arctic Engineering, 2011. American Society of Mechanical Engineers, 637-641.

LIU, Z. & AMDAHL, J. 2019. On multi-planar impact mechanics in ship collisions. *Marine Structures*, 63**,** 364-383.

MOAN, T., AMDAHL, J. & GERHARD, E. 2017. Assessment of ship impact risk to offshore structures-new NORSOK N-003 guidelines. *Marine Structures*.

NORSOK-N003 2017. Action and action effects.

POPOV, Y. N., FADDEEV, O., KHEISIN, D. & YAKOVLEV, A. 1967. Strength of ships sailing in ice. U.S. Army Foreign Science and Technology Center (Translation). .

POPOV, Y. N., FADDEEV, O., KHEISIN, D. & YAKOVLEV, A. 1969. Strength of ships sailing in ice. DTIC Document.

STORHEIM, M. & AMDAHL, J. 2014. Design of offshore structures against accidental ship collisions. *Marine Structures*, 37**,** 135-172.

YU, Z. & AMDAHL, J. 2018a. Analysis and design of offshore tubular members against ship impacts. *Marine Structures*, 58**,** 109-135.

YU, Z. & AMDAHL, J. 2018b. A review of structural responses and design of offshore tubular structures subjected to ship impacts. *Ocean Engineering*, 154**,** 177-203.

YU, Z., AMDAHL, J., RYPESTØL, M. & CHENG, Z. 2021. Numerical modelling and dynamic response analysis of a 10 MW semi-submersible floating offshore wind turbine subjected to ship collision loads. *submitted to journal*.

YU, Z., AMDAHL, J. & SHA, Y. 2018. Large inelastic deformation resistance of stiffened panels subjected to lateral loading. *Marine Structures*, 59**,** 342-367.